

# The Novel Plant Homeodomain Protein Rhinoceros Antagonizes Ras Signaling in the *Drosophila* Eye

Matthew G. Voas<sup>1</sup> and Ilaria Rebay<sup>2</sup>

Whitehead Institute for Biomedical Research and Department of Biology, Massachusetts Institute of Technology, Cambridge, Massachusetts 02142

Manuscript received May 22, 2003  
Accepted for publication September 2, 2003

## ABSTRACT

The sequential specification of cell fates in the *Drosophila* eye requires repeated activation of the epidermal growth factor receptor (EGFR)/Ras/MAP kinase (MAPK) pathway. Equally important are the multiple layers of inhibitory regulation that prevent excessive or inappropriate signaling. Here we describe the molecular and genetic analysis of a previously uncharacterized gene, *rhinoceros* (*mo*), that we propose functions to restrict EGFR signaling in the eye. Loss of *mo* results in the overproduction of photoreceptors, cone cells, and pigment cells and a corresponding reduction in programmed cell death, all phenotypes characteristic of hyperactivated EGFR signaling. Genetic interactions between *mo* and multiple EGFR pathway components support this hypothesis. *mo* encodes a novel but evolutionarily conserved nuclear protein with a PHD zinc-finger domain, a motif commonly found in chromatin-remodeling factors. Future analyses of *mo* will help to elucidate the regulatory strategies that modulate EGFR signaling in the fly eye.

**I**N the developing central nervous system (CNS), the establishment of cell fates appears to be controlled by a clock-like mechanism that progresses with the cell cycle. In the vertebrate brain, neurons born in the proliferating ventricular zone migrate to more superficial positions and differentiate (reviewed in McCONNELL 1989). As development progresses, later-born neurons must migrate past earlier-born neurons before differentiating, resulting in the formation of layers that are arranged by birth date. Furthermore, each layer is composed of different types of neurons, emphasizing the direct correlation between the birth date of a neuron and its fate. While little is known about the molecular basis of this phenomenon in vertebrates, recent advances have been made in the study of a similar process in the fruit fly, *Drosophila melanogaster*. In this case the neural stem cell, referred to as the neuroblast, changes its expression profile of at least four transcription factors as mitosis continues. By manipulating the expression of these factors, the specific type of ganglion mother cell (GMC) born after each division can be controlled (ISSHIKI *et al.* 2001). These data suggest an evolutionarily conserved mechanism for coordinating temporal and spatial information during neuronal determination and provide a useful framework for considering cell fate specification strategies in many different contexts.

The *Drosophila* eye is a neural tissue in which the

mechanisms of cell fate specification have been studied extensively. Research has shown that after each eye facet (called an ommatidium) is established with the selection of the R8 photoreceptor, the epidermal growth factor receptor (EGFR)/Ras/mitogen-activated protein kinase (MAPK) pathway (referred to here as the Ras pathway) is necessary for the specification of all other cell types (FREEMAN 1996, 1997). This occurs through a reiterating mechanism by which cells specified early secrete an EGFR ligand that recruits later-arising cell fates. For example, the R8 photoreceptor secretes the EGF-like ligand Spitz, resulting in the activation of EGFR in the presumptive R2 and R5 photoreceptors. All three photoreceptors then secrete Spitz, allowing the recruitment of R3 and R4, then R1 and R6, and last, R7. Spitz produced by the photoreceptors induces the nonneural cone cells (FREEMAN *et al.* 1992a; FREEMAN 1994b; TIO *et al.* 1994; TIO and MOSES 1997; LEE *et al.* 2001; URBAN *et al.* 2001). In turn, the cone cells are necessary for recruitment of the 1° pigment cells, which in turn are required for the recruitment of the 2° and 3° pigment cells. Undifferentiated cells that do not gain access to sufficient levels of Spitz are eliminated by apoptosis (MILLER and CAGAN 1998).

While the importance of the Ras pathway in eye development is well established, it is unclear how the same signaling pathway specifies such a diverse group of cell types. Specificity appears to be achieved in part by coordinating inputs from additional signaling pathways. For example, activation of the Notch receptor in the presumptive R7 and cone cells is required for their specification (COOPER and BRAY 2000; TOMLINSON and STRUHL 2001; TSUDA *et al.* 2002). The R7 fate further necessitates

<sup>1</sup>Present address: Department of Developmental Biology, Stanford University School of Medicine, Stanford, CA 94305.

<sup>2</sup>Corresponding author: Whitehead Institute, Massachusetts Institute of Technology, 9 Cambridge Center, Cambridge, MA 02142.  
E-mail: rebay@wi.mit.edu

the deployment of a second receptor tyrosine kinase (RTK), Sevenless (SEV), to achieve a peak level of Ras activation (FREEMAN 1996). How cell fate specificity is achieved among the other cell types in the eye remains an open question.

Considering the events of cell fate determination in the *Drosophila* eye in the context of a molecular clock-like mechanism provides a useful framework for answering this question (FREEMAN 1997; HAYASHI and SAIGO 2001). The main difference between cell fate specification in the fly eye *vs.* that in the CNS is that changes in the potential of precursor cells are not linked to the cell cycle (DE NOOIJ and HARIHARAN 1995) and thus the classic neural stem cell model does not apply. Instead, an extensive proliferative phase generates a large pool of undifferentiated cells during larval stages (reviewed in WOLFF and READY 1993). Beginning in the late third instar, cells arrest in G<sub>1</sub> and differentiation initiates along the posterior edge of the larval eye imaginal disc and proceeds anteriorly. As the morphogenetic furrow (MF) passes, rows of widely spaced R8 photoreceptors are specified in its wake, initiating the simultaneous assembly of multiple ommatidia. As described above, the sequential presentation of Spitz ligand determines when a cell begins to differentiate. The timing of this stimulation determines which fate the cell adopts. For example, overexpression of the secreted Spitz ligand or expression of a constitutively activated EGFR results in an excess of mature cell types (FREEMAN 1996). The kind of cells overproduced correlates with the timing of transgenic expression: earlier expression gives extra photoreceptors while later expression gives extra cone cells and pigment cells. Given that the same signal initiates differentiation of multiple cell fates, the undifferentiated precursors in the eye must continually undergo changes in their developmental potential.

Due to the constantly changing developmental potential of eye precursor cells, activation of the Ras pathway must be precisely regulated to ensure a proper complement of ommatidial cells. Such control arises from a finely tuned balance between stimulatory and inhibitory signals (reviewed in FREEMAN 2000; REBAY 2002). For example, a negative feedback loop whereby the EGF-like ligand Argos is produced in response to Ras pathway activation provides an important source of regulation (GOLEMBO *et al.* 1996). Argos binds to EGFR and prevents it from dimerizing, effectively blocking activation (SCHWEITZER *et al.* 1995; JIN *et al.* 2000). The overproduction of all eye cell fates observed in *argos* (*aos*) mutants exactly phenocopies the consequences of expressing activated EGFR (FREEMAN *et al.* 1992b). Conversely, overexpression of *aos* blocks differentiation. Again, the types of cells affected correlate with the time of overexpression (FREEMAN 1994a). Thus, Argos appears to be an important, non-cell-autonomous factor that regulates cell fate specification in the eye.

Here we describe defects in the specification of eye

cell fates in mutant alleles of the *rhinoceros* (*rno*) gene. These defects include the overproduction of R3/R4-like photoreceptors, cone cells, and pigment cells as well as a corresponding reduction in apoptosis in the pupal eye disc. All of these phenotypes are suggestive of a failure to restrict Ras pathway signaling. The overproduction of multiple cell types in *rno* mutant eye clones can occur through a non-cell-autonomous mechanism. Strong genetic interactions between alleles of *rno* and *argos* are consistent with *rno* and *argos* functioning together in a genetic pathway restricting Ras pathway activation. We have molecularly identified the *rno* locus and find that it encodes a plant homeodomain (PHD) class zinc-finger motif-containing protein that is localized to the nucleus. PHD domains are frequently found in chromatin-remodeling proteins (AASLAND *et al.* 1995), suggesting that RNO may function as a nuclear transcription factor. Together these data indicate that *rno* functions as a novel negative regulator of the EGFR pathway in the fly eye and lead to a model whereby *rno* restricts Ras pathway activation by regulating transcription of key pathway regulators.

## MATERIALS AND METHODS

***Drosophila* lines:** *GMR-EbiN* and *Actin>CD2>Gal4, UAS-mCD8-GFP* are from the lab of L. Zipursky. *TM3,sev-Ras<sup>112</sup>* (*T<sub>2</sub>B*) is from the lab of G. Rubin. *l(3)rH321, Sb,P{Δ2-3}99B, TM6B, Ubi-GFP, w<sup>1118</sup>, eyeless-FLP, GMR-lacZ, M(3)Rps17<sup>4</sup>, P{w+}70C, FRT80B/TM6B, P{Ubi-GFP}61E-F, FRT80B, svp<sup>07842</sup>, aos<sup>Δ7</sup>, aos<sup>05845</sup>, 2xUAS-aos*, and *sev-Gal4* (line K24) were acquired from the Bloomington Stock Center. *GMR-Gal4* is from the lab of M. Freeman. The *aos<sup>Δ7</sup>* allele is a predicted protein null as it deletes the first exon that includes the initial methionine codon and the following 121 amino acids (aa; FREEMAN *et al.* 1992b; ADAMS *et al.* 2000).

**Isolation of *rno* alleles:** EMS-induced mutations were generated by feeding isogenized *w<sup>1118</sup>* males 25 mM EMS (Sigma, St. Louis) in 10 mM Tris, pH 7.5 and 1% sucrose for 12 hr at room temperature. Mutagenized males were batch crossed to *TM3/TM6B* virgins, and F<sub>1</sub> male progeny were crossed individually to one of two deficiency lines that uncover *rno*: *Df(3L)XZB970* or *Df(3L)XKR845* (REBAY *et al.* 2000). F<sub>2</sub> progeny were screened for lethal noncomplementation of the deficiency.

**Removal of secondary mutations:** *rno* alleles were recombined onto a multiply marked third chromosome (*h, th, st, cu, sr, e, ca*). The markers were then removed by recombination with a wild-type chromosome. All experiments described here were performed with a "cleaned" allele.

**Generation of mutant eye clones:** For the examination of clones in adult and pupal eyes, *rno, FRT80B/TM6B* or *aos<sup>Δ7</sup>, FRT80B/TM6B* males were crossed to *w<sup>1118</sup>, eyeless-FLP, GMR-lacZ, M(3)Rps17<sup>4</sup>, P{w+}70C, FRT80B/TM6B*. *M(3)Rps17<sup>4</sup>* is a dominant *Minute* mutation that allows homozygous mutant clones to grow faster than neighboring wild-type tissue (NEWSOME *et al.* 2000). Adult eyes were fixed, embedded in plastic, sectioned, and mounted as described (WOLFF 2000). Mutant tissue was recognizable by the absence of red eye pigment (XU and RUBIN 1993). For larval eye disc clones *rno, FRT80B/TM6B* was crossed to *w<sup>1118</sup>, eyeless-FLP; P{Ubi-GFP}61E-F, FRT80B*. Mutant clones were recognizable by the absence of green fluorescent protein fluorescence. For all experiments, control wild-type clones were generated. For pupal clones,

white prepupae were marked and aged at 20° before dissection. For larval clones, larvae were grown at 25°. The *Tb* marker on *TM6B* allowed the unambiguous genotyping of pupae and larvae.

**Immunohistochemistry:** Fixation and antibody staining of S2 cells were performed essentially as described (FEHON *et al.* 1990). Fixation and antibody staining of larval eye discs and pupal retinas were performed essentially as described (WOLFF 2000). The following primary antibodies and concentrations were used: mouse anti-Cut (mAb 2B10, 1:100; G. M. Rubin), rabbit anti-SALM (1:200; R. Barrio), mouse anti-Rough (mAb 62C2A8, 1:100; G. M. Rubin), mouse anti-ARM [mAb N2 7A1, 1:100; Developmental Studies Hybridoma Bank (DSHB)], mouse anti-Argos (mAb 85/2/16, 1:10; DSHB), and mouse anti-ELAV (9F8A9, 1:100; DSHB). Secondary antibodies conjugated to HRP, CY2, or CY3 (Jackson ImmunoResearch, West Grove, PA) were used at concentrations of 1:1000–2000. For all experiments, wild-type control clones were tested alongside *mo* mutant eye clones.

**Acridine orange staining:** Pupal eyes of exactly 50 hr were dissected and incubated in 1 mM acridine orange (Sigma) in PBS for 5 min, rinsed, and then mounted in PBS and photographed immediately.

**Cell counts:** Data found in Tables 1–3 were acquired as follows. For Tables 1 and 2, photoreceptor numbers were determined by examination of adult retinal sections. Ommatidia with at least one homozygous mutant photoreceptor were scored. For Table 3, photoreceptor numbers were determined by counting the number of ELAV-positive nuclei per ommatidium by scrolling through a Z-stack series of confocal images of a larval eye disc. Numbers of cone cells and 1° pigment cells were determined by examination of pupal retinas (60 hr after pupariation at 20°) stained with anti-ARM. To determine numbers of 2° and 3° pigment cells in Table 2 and the number of interommatidial cells in Table 3, hexagonal cell areas were defined around a central ommatidium as described (WOLFF and READY 1991). The number of interommatidial cells in this area is equivalent to the complement for three ommatidia. Cells straddling a boundary were scored as 0.5. A marker was not used to distinguish between mutant and wild-type tissue in pupal eye clones because the presence of a *Minute* allele on the wild-type chromosome generated very large homozygous mutant eye clones (see generation of mutant eye clones above). The unavoidable scoring of some genotypically wild-type ommatidia means that the numbers of cone and pigment cells in *mo*<sup>2</sup> clones are likely to be underestimated in Table 2.

**Generation of excision lines and PCR mapping of deficiency breakpoints:** The *l(3)rH321* insertion is dominantly marked by a *ry*<sup>+</sup> transgene. This line was crossed to *Sb, P{2-3}99B. l(3)rH321/Sb, P{2-3}99B* males were crossed to *TM2,ry/TM6B,ry* virgins and rosy-eyed males and virgins were recovered in the next generation and used to establish a stock. A total of 90 lines were established, one-third of which are alleles of *mo*. For breakpoint mapping, PCR amplification of genomic DNA from animals homozygous for a given deficiency was performed the same way as the PCR for sequencing of *mo* mutant alleles (described below). Primers were designed to amplify small regions of genomic sequence. Failure to amplify a target genomic sequence was interpreted to mean that the target sequence is uncovered by the deficiency. All genomic DNA templates were tested with a positive control set of primers.

**Sequencing of *mo* mutant alleles:** *mo* alleles were balanced over *TM6B, Ubi-GFP* and then nonfluorescent first instar larvae were collected and mashed in TE plus 25 mM NaCl. These smashes were digested in 200 µg/ml of proteinase K for 30 min at 37° and then heat inactivated at 95° for 2 min. The *mo* locus was PCR amplified in pieces of 500–1000 bp. The same PCR primers were then used to sequence using the Big Dye Terminator kit (ABI, Columbia, MD).

**Construction of a full-length *mo* cDNA:** On the basis of the predicted sequence of *mo* (ADAMS *et al.* 2000), probes of the PHD region of *mo* and the 3' end of *mo* were made by PCR using the following primer pairs. For the PHD region, primers ZFS (5' TGTTCGATGGGAATTAAGCCGGAC 3') and ZFA (5' CTTCTTACCCTTGCTCATACTGTG 3') were used to generate a 386-bp fragment by PCR from a genomic template, while for the 3' end of the *mo*-coding region, primers BOS (5' TGCCTGCTCTTGATGCCAAGCTTAG 3') and BOA (5' TTGATCGAGTTGCTATTGCAGGAG 3') were used to generate a 1206-bp fragment. Radiolabeled probes were made and used to screen filter lifts of λ-phage plaques from the Ling Damon (LD) [poly(dT) primed, 0- to 22-hr embryonic mRNA; G. Rubin] and embryonic random primed (ERP; G. Rubin) libraries. Four 3' probe-hybridizing clones were isolated from the LD library, while two PHD-hybridizing clones were isolated from the ERP library. The cDNAs were recovered by excision of pBluescript plus insert from the λZAP arms (Stratagene, La Jolla, CA). End sequencing revealed that the 5'-most, 2.6-kb clone contains several in-frame stop codons upstream of the predicted reading frame, indicating that the 5' end of the coding region had been recovered. The longest 3' clone was 7.6 kb and contained a poly(A) tail. To join the 5' and 3' clones, a 1.8-kb fragment was reverse transcription (RT)-PCR'd from adult total RNA. A full-length clone was constructed by subcloning a 2.1-kb *NotI/MluI* 5' fragment, a 1.8-kb *MluI/BglII* RT-PCR fragment, and a 7.4-kb *BglII/XhoI* 3' fragment into the *NotI* and *XhoI* sites of pBluescript (Stratagene). The resulting 10,821-bp cDNA was fully sequenced on both strands and compared to the *Drosophila* genome sequence. Several nucleotide polymorphisms between the cloned *mo* cDNA sequence and the reported genomic sequence were found, but none are predicted to alter the amino acid composition.

**Transgenic overexpression of *mo*:** The full-length *mo* cDNA was subcloned into the *NotI/XhoI* sites of the pUAST transformation vector (BRAND and PERRIMON 1993). To add a Myc epitope to the N terminus of RNO, a PCR primer was designed to encode a *NotI* site followed by a Kozac consensus, an ATG, the 11 codons of the Myc epitope, and 18 nucleotides of homology to the 5' end of *mo*, excluding the initial methionine codon (MV48: 5' CAGTGC GGCCG CCAAAAACATGGAGCAA AAGCTCATTCTGAAGAGGACTTGAGGTCACAAAGAGG TAAGCGC 3'). PCR of the 5' end of *mo* using the cDNA as template was performed using oligos MV48 and MV22 (5' GATCGCTGTTGTAGAGACGCA 3'). The product was digested with *NotI* and *SacII* and the resulting 275-bp fragment was subcloned into *NotI/SacII*-digested pUAST-*mo*. The resulting clone, pUAST-*myc-mo*, lacks the 5' untranslated region of *mo*. Sequencing of the PCR-amplified region and the region derived from the oligo MV48 confirmed this construct. QIAGEN-maxiprep plasmid (QIAGEN, Valencia, CA) was injected into embryos to make six transgenic lines by standard techniques. To overexpress *mo* in the eye imaginal disc during third instar, *UAS-myc-mo* was crossed to *sevenless-Gal4* or *GMR-Gal4*. To overexpress *mo* in the eye imaginal disc for several days prior to third instar, a combination of the FLP-out and *UAS/Gal4* systems was employed (PIGNONI and ZIPURSKY 1997). *eyeless-FLP; UAS-myc-mo* flies were crossed to *Actin>CD2>Gal4* to give *eyeless-FLP/Act>CD2>Gal4; UAS-myc-mo* progeny. This allows the gradual accumulation of Myc-RNO protein beginning very early in larval development. This method was not lethal to the larvae, while simply crossing *eyeless-Gal4* to *UAS-myc-mo* killed larvae well before third instar, presumably due to leakiness of the *eyeless* promoter in the brain. To generate clones of cells that overexpress *mo*, *hs-FLP; UAS-myc-mo*, flies were crossed to *Actin>CD2>Gal4, UAS-mCD8-GFP*. At 48 hr after egg deposition, the eggs were heat shocked at 37° for 1 hr.

**Generation of anti-RNO antiserum:** Various regions (700–1200 bp long) of the *rno* cDNA were subcloned into the bacterial expression vector, pGEX-4T (Stratagene). In this way, almost all of the RNO sequence was fused to the C terminus of glutathione-S-transferase (GST) in pieces of 234–401 aa (12 fusions total). Of these fusions, 4 showed sufficiently high expression to purify enough soluble protein for injection into mice (REBAY and FEHON 2000). Bleeds were tested against *Drosophila* S2 cells transfected with *Ubiquitin-Gal4*, *UAS-rno* at concentrations ranging from 1:500 to 1:10,000. Two of the 4 fusions generated antiserum that could recognize nuclear RNO in transfected S2 cells. The better antiserum (referred to here as anti-RNO) recognizes aa 2607–2853.

## RESULTS

***rno* restricts differentiation in the eye non-cell autonomously:** A lethal noncomplementation screen was performed to induce EMS mutations in a putative positive RTK pathway gene, provisionally referred to as *EY3-5*, which we had identified in a previous genetic screen (REBAY *et al.* 2000). Because the original *EY3-5* alleles were both deficiencies uncovering chromosomal band region 61A–B (REBAY *et al.* 2000), several complementation groups were recovered from the F<sub>2</sub>-lethal screen, one of which we have named *rhinoceros* (*rno*). *EY3-5* and *rno* do not appear to be the same gene on the basis of complementation tests and opposite direction of interactions with RTK pathway components (this work; REBAY *et al.* 2000; data not shown). However, *rno* mutants showed eye phenotypes suggestive of a role in developmental regulation of eye cell fates that led us to pursue its characterization (see below).

Using the FLP/FRT technique for mitotic recombination (XU and RUBIN 1993), clones of eye and antennal tissue homozygous for *rno* were generated. In the antenna, *rno* mutant clones produce a highly penetrant transformation of the arista to a leg-like appendage (Figure 1, A and B). The appearance of these horn-like structures on the head led us to name the gene *rhinoceros*. While the aristapedia phenotype was not investigated further, examination of *rno* clones in adult eyes reveals the presence of extra photoreceptors (Figure 1, C and D), predominantly of the R1–R6 class (“outer” photoreceptors). This extra photoreceptor phenotype has been observed in six independent *rno* alleles. Further analysis of three of these alleles shows that the frequency of homozygous mutant ommatidia with one extra outer photoreceptor ranges from 30 to 38% (Table 1). Less frequently, ommatidia that have an extra R7 or more than one extra photoreceptor are seen (Table 1). The average number of photoreceptors per ommatidium in *rno2* eye clones is 8.4, compared to 8.0 for wild-type control clones (Table 2). Some affected ommatidia that are composed entirely of genotypically wild-type R cells were observed (Figure 1E). The occurrence of phenotypically mutant ommatidia that are genotypically wild type demonstrates that the extra pho-

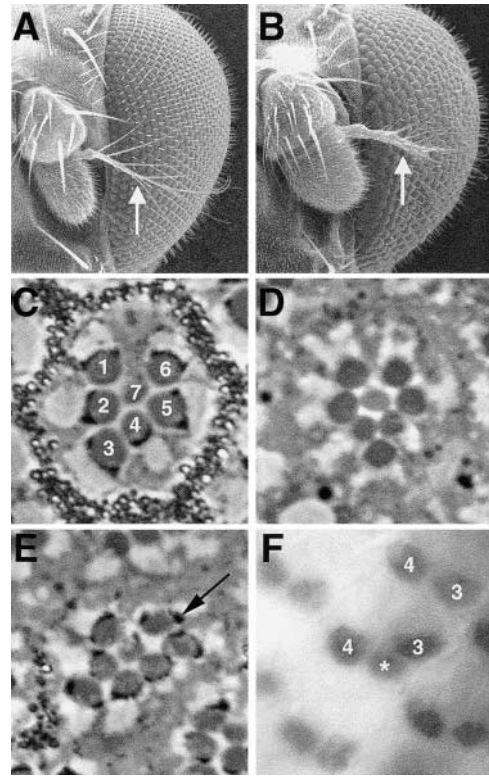


FIGURE 1.—Loss of *rno* function results in aristapedia and the overproduction of photoreceptors. (A) In a wild-type control clone, the arista has a normal, feather-like appearance (white arrow). (B) In this *w<sup>1118</sup>*, *ey-FLP/+*; *rno<sup>2</sup>*, *FRT80B/RpS17<sup>4</sup>*, *P{w<sup>+</sup>}*, *FRT80B* fly, the formation of *rno* mutant clones in the antenna causes a transformation of the arista to a leg-like structure (white arrow). (C) The stereotyped arrangement of photoreceptors in an adult wild-type ommatidium. The rhabdomeres are labeled with their corresponding R cell number. R8 is not visible in this plane of section. (D) A homozygous mutant ommatidium from an adult of genotype *w<sup>1118</sup>*, *ey-FLP/+*; *rno<sup>1</sup>*, *FRT80B/RpS17<sup>4</sup>*, *P{w<sup>+</sup>}*, *FRT80B*. An extra outer photoreceptor is present. (E) Another ommatidium from a *w<sup>1118</sup>*, *ey-FLP/+*; *rno<sup>1</sup>*, *FRT80B/RpS17<sup>4</sup>*, *P{w<sup>+</sup>}*, *FRT80B* fly. The presence of dark pigment granules associated with the edge of each rhabdomere (arrow) indicates that all the photoreceptors are genotypically wild type, yet the ommatidium displays the *rno* mutant phenotype. (F) R3 and R4 nuclei from a *w<sup>1118</sup>*, *ey-FLP/+*; *rno<sup>2</sup>*, *FRT80B/RpS17<sup>4</sup>*, *P{w<sup>+</sup>}*, *FRT80B* larval eye disc are stained with anti-SALM. In the top right-hand corner the R3 and R4 nuclei of a phenotypically wild-type ommatidium are indicated. In the middle is an affected ommatidium. The presence of an ectopic SALM-positive nucleus (\*) can be clearly seen between R3 and R4. The occurrence of an ectopic photoreceptor in this position is consistent with the transformation of a mystery cell to an R3/R4.

photoreceptor phenotype can occur through a non-cell-autonomous mechanism.

To determine the identity of the extra R cells, third instar larval eye discs bearing *rno* mutant clones were probed with cell-type-specific markers. Using the R3/R4 marker anti-SALM, ommatidial clusters that contain three SALM-positive nuclei were observed (Figure 1F). The extra photoreceptor tended to occur between the

TABLE 1

Loss of *mo* increases photoreceptor number

Phenotype of ommatidia	WT	<i>mo</i> <sup>1</sup>	<i>mo</i> <sup>2</sup>	<i>mo</i> <sup>3</sup>
% wild type	99.2	52.7	56.2	59.0
% +1 outer R cell	0.1	37.8	32.5	30.2
% +1 R7	0.0	2.6	2.4	1.1
% +2 or more R cells	0.0	5.8	5.3	4.6
% -1 or more R cells	0.7	1.1	3.6	5.1
Total ommatidia scored	1149	617	1000	807

Ommatidia from homozygous *mo* eye clones or wild-type (WT) control clones were scored for the number and type of photoreceptors present. See MATERIALS AND METHODS for details.

R3 and R4 photoreceptor. This position is occupied by two "mystery" cells per ommatidium (WOLFF and READY 1993), so the ectopic photoreceptors observed in *mo* mutant clones may arise from transformed mystery cells. The normal fate of the mystery cells is unknown, so exactly what kind of transformation event this might represent is unclear. Extra R3/R4-like nuclei were also observed in *mo* clones in the mid-pupal retina, using a *seven-up-lacZ* enhancer trap (data not shown). Extra R2/R5 cells were never observed on the basis of expression of the marker Rough (data not shown). Thus, the ectopic outer photoreceptors are of the R3/R4 type.

To investigate the origin of the extra R3/R4 photoreceptors, we asked whether any other cell fates are affected in *mo* eye clones. If the extra R3/R4 neuron results from a cell fate transformation, then there should be a concomitant loss of another cell type. On the other hand, if other cell types appear unaffected or are even increased in number, then the extra cells are most likely drawn from the pool of undifferentiated cells that surround the ommatidial center in the late larval and pupal eye disc. Because differentiation of the photoreceptor neurons, apart from induction of an ectopic R3/R4-like cell, appears normal in *mo* mutants, we focused these analyses on the nonneuronal cell types. To test for the presence of either missing or ectopic cone cells, pupal eye clones were tested for expression of the nuclear cone cell marker, Cut. In *mo* pupal eye clones, many ommatidia contain one extra Cut-positive nucleus relative to the normal complement of four seen in wild-type control clones (Figure 2, A and B). Labeling of the cell plasma membranes reveals the presence of extra cone and pigment cells (Figure 2, C and D). By counting the numbers of cone and pigment cells, it was found that *mo* mutant eye clones contain 4.4 cone cells, 2.2 1° pigment cells, and 5.3 2°/3° pigment cells per ommatidium while wild-type control clones contain 4.0, 2.0, and 4.0, respectively (Table 2). Including the photoreceptors, the total number of cells per ommatidium is 18.0 for the wild type and on average 20 for *mo* mutant clones (Table 2). From these analyses, it appears that

TABLE 2

Multiple cell fates are overproduced in *mo* mutant eye tissue

	WT	<i>mo</i> <sup>2</sup>
Photoreceptors	8.0 ± 0.1 (1149)	8.4 ± 0.6 (1000)
Cone cells	4.0 ± 0.1 (146)	4.4 ± 0.7 (143)
1° pigment cells	2.0 ± 0.1 (146)	2.2 ± 0.4 (143)
2° and 3° pigment cells	4.0 ± 0.0 (10)	5.3 ± 0.3 (10)
Total of averages	18.0 ± 0.2	20.3 ± 1.0

Average numbers of cells per ommatidium are shown with the standard deviations. For photoreceptors, cone, and 1° pigment cells, the numbers of ommatidia scored are in parentheses. For 2° and 3° pigment cells, the numbers of cell areas scored are shown. See MATERIALS AND METHODS for details. The R8 photoreceptor was not explicitly scored. However, the presence of one R8 per ommatidium can be assumed because each ommatidium is founded by an R8.

multiple cell fates are overproduced in *mo* mutant eye tissue and that these ectopic cells do not arise from cell fate transformations but are most likely recruited from the pool of undifferentiated cells.

In the mid- to late-pupal retina, any remaining undifferentiated cells are eliminated by apoptosis (WOLFF and READY 1993). If the extra photoreceptors, cone cells, and pigment cells seen in *mo* mutant eye tissue are derived from these undifferentiated cells, then there should be a reduction in programmed cell death in the pupal retina. When flies are raised at 20°, the peak of cell death in the wild-type retina occurs at 50 hr after puparium formation (APF; WOLFF and READY 1993). At 50 hr APF, wild-type control clones show strong staining with the apoptotic dye acridine orange (Figure 2, E and F). However, acridine orange staining in *mo* pupal eye clones is dramatically reduced (Figure 2, G and H). This result indicates that fewer undifferentiated cells are dying in *mo* mutant eye clones, most likely because they acquire cell fates and are incorporated into the mature ommatidia.

***mo* interacts genetically with the Ras pathway:** The overproduction of multiple cell types and reduced cell death phenotypes observed in *mo* mutant eye tissue suggest that *mo* may function as an antagonist of the Ras pathway. Of the known Ras pathway antagonists such as *aos*, *Gap1*, *yan*, and *tramtrack (ttk)*, only *aos* mutants have been shown to result in the overproduction of all cell fates in a non-cell-autonomous manner (FREEMAN *et al.* 1992b; GAUL *et al.* 1992; LAI and RUBIN 1992; LAI *et al.* 1996). To explore the possibility that *mo* and *aos* function in the same genetic pathway, alleles of *mo* were tested for their ability to dominantly enhance an *aos* mutant eye phenotype. In *aos*<sup>Δ7</sup>/*aos*<sup>05845</sup> hypomorphic escaper flies, extensive blistering occurs along the posterior edge of the eye (Figure 3, A and B). This phenotype has also been observed in *aos*<sup>W11</sup>/*aos*<sup>W11</sup> escaper flies and results from massive overrecruitment of cone cells in

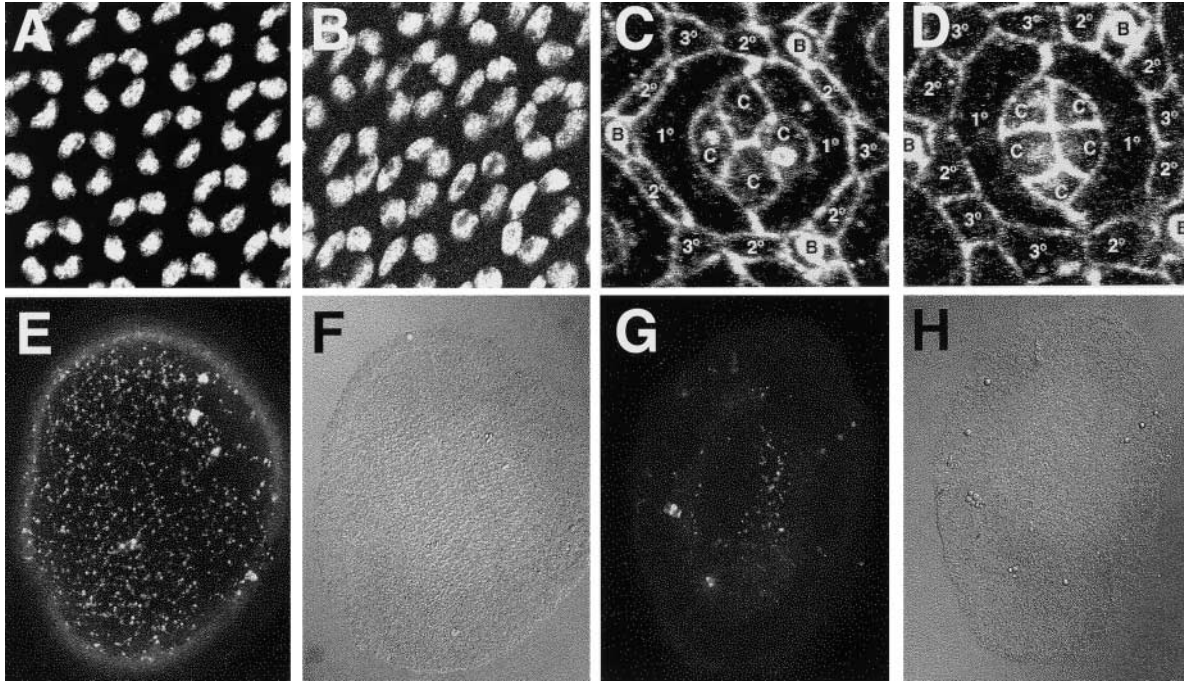


FIGURE 2.—*mo* eye clones overproduce cone and pigment cells and have reduced apoptosis. (A) A wild-type control eye clone at 40 hr APF stained with anti-Cut. The distinctive arrangement of four cone cell nuclei per ommatidium is seen. (B) Bristle. A similar eye clone from a *w<sup>1118</sup>, ey-FLP/+; mo<sup>3</sup>, FRT80B/RpS17<sup>4</sup>, P{w<sup>+</sup>}, FRT80B* pupa. Several ommatidia contain five Cut-positive nuclei. (C) Cone cell. 1°, 2°, 3°: pigment cells. An ommatidium from a wild-type control clone stained with anti-ARM at 60 hr APF. The normal cell membrane morphology is clearly visible. (D) An ommatidium from a pupa of genotype *w<sup>1118</sup>, ey-FLP/+; mo<sup>2</sup>, FRT80B/RpS17<sup>4</sup>, P{w<sup>+</sup>}, FRT80B* at 60 hr APF. There is one additional cone cell and two additional 3° pigment cells (here a 3° pigment cell is considered an interommatidial cell that does not contact a bristle). Note that the 2°/3° pigment cell lattice does not narrow as is seen in the wild type at this stage. This morphological defect has been observed as late as 70 hr APF (data not shown). (E) A wild-type control clone stained with acridine orange shows a normal intensity of staining at 50 hr APF. (F) Nomarski image of the retina in E. (G) A 50 hr APF pupal retina of the genotype *w<sup>1118</sup>, ey-FLP/+; mo<sup>2</sup>, FRT80B/RpS17<sup>4</sup>, P{w<sup>+</sup>}, FRT80B* stained with acridine orange. Staining is drastically reduced compared to the wild-type control, indicating that apoptosis is largely absent. (H) Nomarski image of the retina in G.

this position (FREEMAN *et al.* 1992b). Tests with three independent *mo* alleles reveal that in *mo/+*, *aos<sup>Δ7</sup>/aos<sup>05845</sup>* flies, the blistering becomes more pronounced and extends to the anterior regions of the eye (Figure 3C). This strong genetic interaction suggests that *mo* and *aos* function in the same pathway.

To test further the hypothesis that *mo* functions antagonistically to the EGFR/Ras/MAPK pathway, additional genetic and molecular tests were performed. For example, an eye phenotype caused by the expression of a constitutively active isoform of Ras (*Ras<sup>V12</sup>*) is dominantly enhanced by alleles of *mo* (two alleles tested) as would be expected for a negative regulator (Figure 3, D and E). This interaction is similar to that seen between the *Ras<sup>V12</sup>* phenotype and *aos<sup>Δ7</sup>* (Figure 3F). In addition, heterozygosity for *mo* (four alleles tested) dramatically suppresses the rough eye phenotype associated with expression of a dominant negative isoform of the F-box protein Ebi (*EbiN*; Figure 3, G–I). Ebi functions downstream of EGFR signaling in the targeted degradation of the transcription factors and pathway antagonists Tramtrack88 and Su(H) (DONG *et al.* 1999; TSUDA *et al.*

2002). Thus suppression of a dominant negative Ebi phenotype is again consistent with a role for *mo* as a negative regulator of the pathway.

Because *mo* mutants are homozygous lethal, dying as late embryos or early first instar larvae, we asked whether the embryonic phenotypes might be similarly indicative of EGFR pathway hyperactivation. First we examined the cuticles of the dead embryos/larvae, looking for an example of lateral spacing defects observed in *aos* zygotic mutants (FREEMAN *et al.* 1992b), but found no obvious abnormalities (data not shown). Further examination with a variety of markers failed to reveal any neuronal, axonal, or glial defects that might indicate hyperactive EGFR signaling (data not shown). Because *in situ* hybridization studies suggested that *mo* is maternally deposited (data not shown), we investigated the consequences of removing both maternal and zygotic *mo*. However, in our hands, the stocks for generating germline clones of genes on 3L, obtained from several independent sources and used with multiple *mo* alleles, did not yield reproducible results, thwarting this analysis. Thus it remains to be determined how specific or

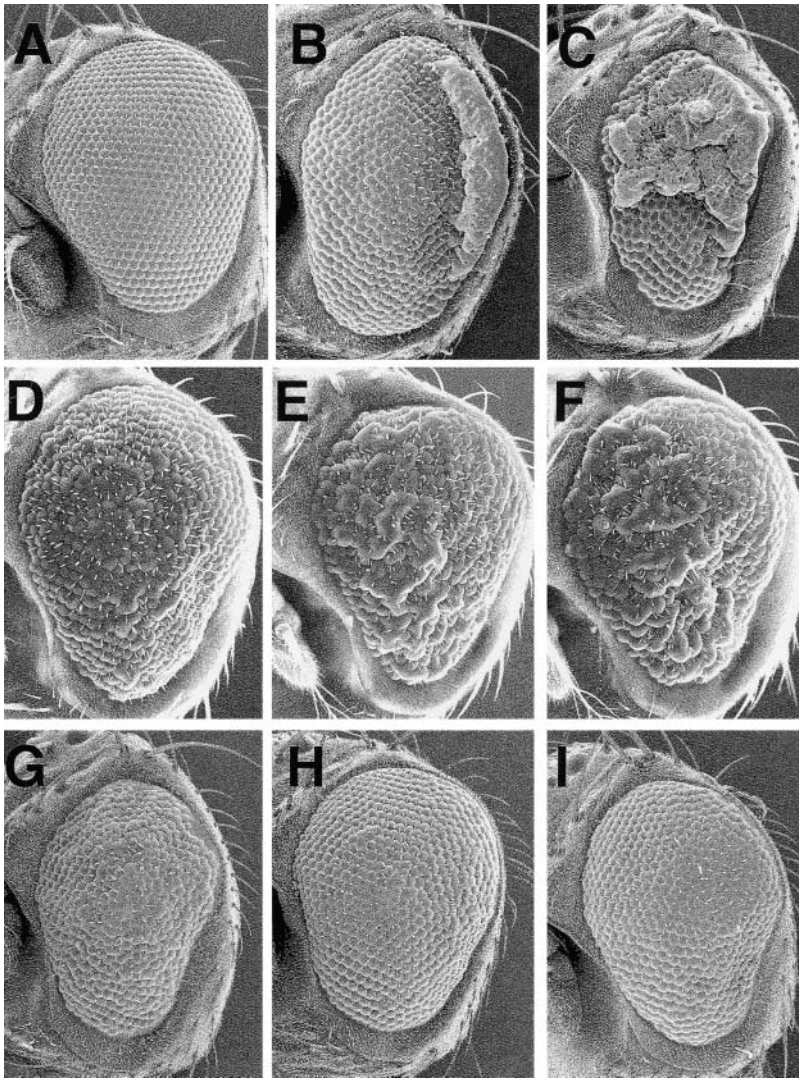


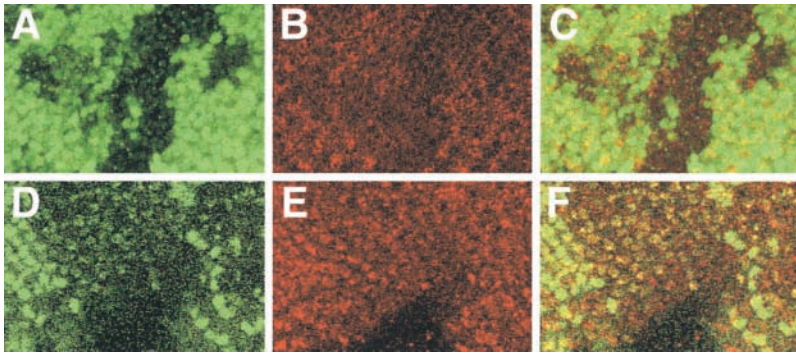
FIGURE 3.—Alleles of *mo* interact with components of the Ras pathway. Scanning electron micrographs of adult eyes are shown. (A) Wild type. In this and all other frames, anterior is to the left. (B) *aos<sup>Δ7</sup>/aos<sup>05845</sup>*. Note the extensive blistering along the posterior edge. (C) *mo<sup>3</sup>, aos<sup>Δ7</sup>/+, aos<sup>05845</sup>*. The blistering in this eye is much more severe than in B and extends to the anterior edge. (D) *TM3-sev-Ras<sup>V12</sup>/+*. The surface of the eye is rough due to numerous small blisters and other abnormalities. (E) *TM3-sev-Ras<sup>V12</sup>/mo<sup>2</sup>*. The rough eye phenotype is dramatically enhanced with much larger regions of blistering. (F) *TM3-sev-Ras<sup>V12</sup>/aos<sup>Δ7</sup>*. The rough eye phenotype is enhanced. This enhancement is comparable to that seen in E. (G) *GMR-EbiN/GMR-EbiN* has a small, roughened eye. (H) *GMR-EbiN/GMR-EbiN; mo<sup>2</sup>/+*. The eye is restored to wild-type size and the roughness is drastically suppressed. (I) *GMR-EbiN/GMR-EbiN; mo<sup>5</sup>/+* also shows strong suppression of the eye phenotype.

general *mo*'s role as an EGFR pathway antagonist is during development.

**Argos expression may be slightly reduced in *mo* mutant eye clones:** The non-cell-autonomous phenotype of *mo* and the strong genetic interaction between *mo* and *aos* led us to investigate whether production of the Argos ligand might be compromised in *mo* mutant tissue in the developing eye. We assayed Argos expression using a previously generated monoclonal anti-Argos antibody (FREEMAN 1994a). In the third instar larval eye disc, staining with this antibody can be seen beginning in the MF and extending posteriorly (Figure 4B; SPENCER *et al.* 1998). This punctate expression pattern is consistent with a protein that is expected to be present in secretory vesicles. Furthermore, the specificity of this pattern was demonstrated by the reduction of staining in *aos<sup>Δ7</sup>* larval eye clones (Figure 4, A–C). When larval eye clones of *mo* were probed with anti-Argos, staining in *mo* mutant tissue appeared slightly reduced (Figure 4, D–F, two alleles tested). Reduced Argos expression

in *mo* mutant eye tissue is consistent with a function for *mo* as a Ras pathway antagonist, although the molecular mechanism underlying the interaction between *mo* and *aos* remains to be elucidated.

***mo* encodes a putative chromatin-remodeling factor:** Alleles of *mo* fail to complement *Df(3L)XZB970*, which uncovers ~400 kb of band region 61A–B (data not shown; REBAY *et al.* 2000). A *P*-element insertion associated with an ~50-kb deletion, referred to here as *Df(3L)rH321*, lies within this region and complements alleles of *mo*. Expansion of the *Df(3L)rH321* deletion was accomplished by imprecise excision of the *l(3)rH321* insertion. Among the new deficiency lines generated was *Df(3L)rH321Δ26*, which fails to complement *mo*. *Df(3L)rH321Δ26* has the same proximal breakpoint as *Df(3L)rH321*, but its distal breakpoint lies ~5 kb beyond that of *Df(3L)rH321* (Figure 5A). Only one predicted gene, CG7036, lies within this region (ADAMS *et al.* 2000). By sequencing the CG7036 locus, eight *mo* alleles were found to contain nonsense mutations (*mo<sup>2</sup>* was



type tissue. (E) Anti-Argos staining. There is a slight reduction of Argos expression in the homozygous mutant tissue. (F) Merged image of D and E. For all frames, posterior is up and the bottom edge of each frame is posterior to the MF.

FIGURE 4.—Argos production is reduced in *rno* mutant clones. (A–C) A third instar larval eye disc of the genotype *ey-FLP; aos $\Delta$ 7, FRT80B/Ubi-GFP, FRT80B*. (A) Green fluorescent protein (GFP) fluorescence marks wild-type tissue. Note that fluorescence from homozygous wild-type tissue is more intense than that from heterozygous wild-type tissue. (B) Anti-Argos staining. In the wild-type tissue, there is a punctate expression pattern. The loss of staining in the homozygous *aos $\Delta$ 7* mutant clone confirms the specificity of the antibody. (C) Merged image of A and B. (D–F) Larval eye disc of the genotype *ey-FLP; rno $^3$ , FRT80B/Ubi-GFP, FRT80B*. (D) Green fluorescence marks the wild-

recovered twice; Figure 5A). None of these sequence substitutions occurs in the wild-type stock from which the *rno* alleles were derived. This result confirms that CG7036 is the same as *rno*.

The predicted RNO protein is 3241 amino acids long. Motif analysis using Pfam (BATEMAN *et al.* 2002) reveals the presence of a C<sub>4</sub>HC<sub>3</sub> PHD class zinc-finger motif near the amino terminus of RNO (Figure 5; AASLAND *et al.* 1995; SAHA *et al.* 1995). The PHD finger is followed by a zinc-finger-like structure commonly found following PHD fingers that has been referred to as a cysteine-rich region (SAHA *et al.* 1995) or an extended PHD finger (Figure 5B; LINDER *et al.* 2000). The extended PHD finger contains 13 conserved cysteines and histidines, 8 of which are arranged in a pattern reminiscent of a PHD finger in which the final cysteine is replaced with a histidine (C<sub>4</sub>HC<sub>2</sub>H; Figure 5B). A TBLASTN search for related proteins in *D. pseudoobscura* (<http://www.hgsc.bcm.tmc.edu/projects/drosophila/>) and in the mosquito, *Anopheles gambia* (HOLT *et al.* 2002), reveals that the orthologous proteins are 3369 and 4120 aa long, respectively. Comparison between *Drosophila* and *Anopheles* RNO shows that the N terminus is highly conserved (62% identical and 72% similar, Figure 5B). This region is also highly conserved in three human proteins, KIAA0215 (46% identical, 61% similar), JADE-1 (44% identical, 62% similar), and KIAA0239 (40% identical, 57% similar; Figure 5B), as well as in related proteins in the mouse, rat, zebrafish, and sea squirt (data not shown). Outside of this N-terminal region, *Drosophila* and *Anopheles* RNO contain short and widely spaced blocks of conserved sequence, along with nonconserved stretches of low complexity sequence, such as polyserine and polyglutamine (Figure 5A). These long, repetitive tails are absent in the human proteins. The stop codons found in *rno<sup>1</sup>* and *rno<sup>2</sup>* are predicted to truncate RNO before the PHD finger, suggesting that these alleles may be nulls (Figure 5A). More than 750 proteins containing PHD fingers have been found in a wide variety of species (MULDER *et al.* 2003). Most frequently, they occur in the subunits of chromatin-remodeling complexes (AAS-

LAND *et al.* 1995). Biochemically, they have been shown to act as protein-protein interaction domains by binding to other PHD domains or to structurally unrelated motifs (FAIR *et al.* 2001; O'CONNELL *et al.* 2001; KRAMPS *et al.* 2002). The extended PHD domain is likewise capable of binding proteins (LINDER *et al.* 2000). Thus, the PHD domain suggests a role for RNO as part of a chromatin-remodeling complex.

**RNO is a nuclear protein:** To examine the developmental expression and subcellular localization of RNO, polyclonal antiserum was raised against RNO. Strong anti-RNO staining can be detected in the nuclei of S2 cells transfected with an *rno* expression vector (Figure 6, A and B). However, efforts to detect endogenous RNO in the eye imaginal disc with this antiserum have been unsuccessful. To circumvent this problem, the coding region of the Myc epitope was fused upstream of the *rno* cDNA in the pUAST expression vector (BRAND and PERRIMON 1993). When Myc epitope-tagged RNO is transgenically expressed in a subset of cells posterior to the MF using *sevenless-Gal4*, it is easily detected in nuclei with anti-Myc (Figure 6C), but not with anti-RNO (not shown). If Myc-RNO is expressed in the eye imaginal disc for several days before dissection at the third instar stage (see MATERIALS AND METHODS), then anti-RNO can detect nuclear Myc-RNO (Figure 6, D and E). On the basis of these data, it is likely that endogenous RNO protein in the eye imaginal disc is normally present at low levels in the nucleus. This conclusion is consistent with the predicted role of RNO as a member of a chromatin-remodeling complex.

**Overexpression of *rno* causes a degenerative phenotype:** Because *rno* loss-of-function results in overproduction of all multiple types in the eye, we predicted that overexpression of *rno* would lead to a reduced complement of cells in each ommatidium. To test this hypothesis, retinas from *GMR-Gal4; UAS-myc-rno* larvae and pupae were examined for developmental defects. Surprisingly, the average number of photoreceptors and cone cells appeared unaffected, while the number of 1<sup>o</sup> pigment cells was slightly elevated from 2.0 per omma-



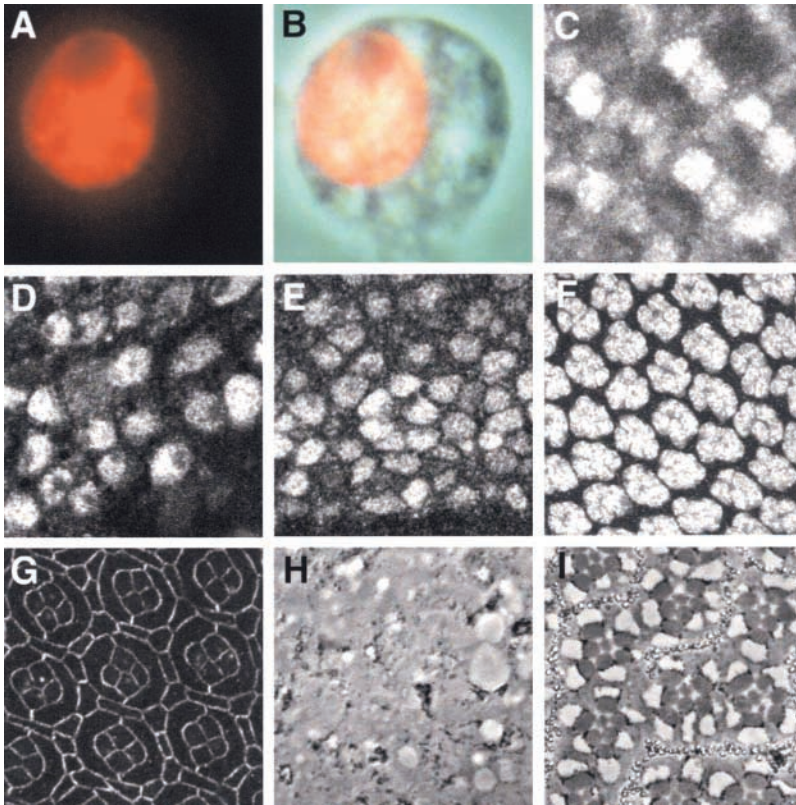


FIGURE 6.—Transgenically expressed RNO localizes to the nucleus and causes a degenerative phenotype. (A and B) *Ubi-Gal4*, *UAS-rno*-transfected S2 cell stained with anti-RNO (A) and merged with a phase-contrast image of the cell (B) clearly shows the nuclear localization of RNO. (C) Imaginal disc of the genotype *sev-Gal4*; *UAS-myc-rno* stained with anti-Myc allows detection of nuclear RNO most strongly in the R3/R4 cells. (D and E) Prolonged overexpression of Myc-RNO in the eye imaginal disc (see MATERIALS AND METHODS) allows anti-RNO to detect nuclear RNO in the peripodium (D) and in cells posterior to the MF (E). (F–H) Overexpression of *rno* in *GMR-Gal4*; *UAS-myc-rno* eye does not affect the specification of photoreceptors (E, larval eye disc stained with anti-ELAV) or the specification of cone cells and 1° pigment cells (G, 60 hr APF pupal eye disc stained with anti-ARM). However, adult flies of this genotype show severe retinal degeneration (H, section of adult retina). The rhabdomeres and the pigment cell lattice that is normally visible (see Figure 1C) have been replaced by vacuoles and scattered pigment granules. (I) Sections of the eye of a *sev-Gal4*; *UAS-myc-rno* adult fly. Extensive loss of pigment cells is apparent while the photoreceptors are less severely affected.

Rather, overexpression of *rno* results in degeneration of the retina well after the majority of the cell types have been recruited. Considering that *rno* regulates cell fate specification events during normal development (Figures 1 and 2), the relevance of overexpression-induced late-onset degeneration with respect to the endogenous function of *rno* is not yet clear.

#### DISCUSSION

The results presented in this article lead us to propose that *rno* restricts the specification of multiple cell fates

TABLE 3

Overexpression of *rno* in the developing eye does not dramatically alter cell fate

Photoreceptors	8.0 ± 0.0 (108)
Cone cells	4.0 ± 0.2 (254)
1° pigment cells	2.1 ± 0.3 (227)
Interommatidial cells	4.3 ± 0.3 (10)

Pupal retinas of genotype *GMR-Gal4/+*; *UAS-myc-rno/+* were scored for the presence of the above cell types. The average numbers of cells per ommatidium are shown with the standard deviations. The numbers of ommatidia scored are in parentheses. Due to the degeneration of the retina before adulthood, the number of photoreceptors was determined by counting the number of ELAV-positive nuclei in the larval eye disc (see MATERIALS AND METHODS for details).

in the *Drosophila* eye by antagonizing the EGFR/Ras signaling pathway. In developing *rno* mutant eye tissue, excess photoreceptors, cone cells, and pigment cells arise. Consistent with these observations, programmed cell death among undifferentiated cells in the midpupal retina is decreased in *rno* mutants relative to wild-type controls. Therefore, the ectopic cells seen in *rno* mutant ommatidia are likely to result from improper recruitment events. These phenotypes are highly suggestive of a role for *rno* in negative regulation of RTK signaling events.

In the eye, phenotypic similarities exist between the *rno* mutant phenotype and that of other Ras pathway antagonists such as *aos*, *Gap1*, *yan*, and *ttk* (FREEMAN *et al.* 1992b; GAUL *et al.* 1992; LAI and RUBIN 1992; LAI *et al.* 1996). Mutation in all of these genes results in supernumerary photoreceptors. Furthermore, loss of *Gap1* also results in extra 1° and 2°/3° pigment cells, while loss of *yan* results in extra cone cells and 1° pigment cells (the effects of *ttk* loss-of-function on cone and pigment cells are unknown). However, the *Gap1*, *yan*, and *ttk* eye phenotypes differ from those of *rno* mutants in that they tend to overproduce many R7-like photoreceptors per ommatidium. The *aos* phenotype is more similar to that of *rno* because in addition to affecting cone cells and all pigment cell types, the ectopic photoreceptors in *aos* mutant eyes are mostly mystery cells that have been transformed into R3/R4 (FREEMAN *et al.* 1992b). The molecular cause of this phenotypic difference between *aos* and other Ras pathway antago-

nists is unknown. Like *yan* and *ttk*, *aos* is broadly expressed (FREEMAN *et al.* 1992b; LAI and RUBIN 1992; LAI *et al.* 1996), so differences in expression pattern cannot be cited. One possible explanation is that as an extracellular ligand that is presumably specific to one RTK, EGFR, the effect of Argos on Ras pathway activity is limited. On the other hand, the actions of Gap1, Yan, and TTK do not have RTK specificity in the developing eye, and as a result, they may be more potent inhibitors of Ras pathway activity within the cell. Differences in specificity may be especially important for R7 determination, which requires stimulation of two RTKs, EGFR and SEV, to achieve high levels of Ras pathway activation (FREEMAN 1996; TIO and MOSES 1997).

The similarity between the *mo* and *aos* eye phenotypes led us to explore whether *mo* operates in the same pathway as *aos*. Supporting this model, we find a strong genetic connection between *mo* and Ras pathway components. First, heterozygosity for *mo* strongly enhances an *aos* eye phenotype. Second, *mo* can dominantly enhance the eye phenotype produced by activated Ras. Third, *mo* can dominantly suppress the rough eye phenotype of a dominant-negative Ebi. Fourth, Argos production appears slightly reduced in *mo* mutant clones, reflecting the insufficient restriction of Ras pathway signaling. Together these results argue strongly that *mo* antagonizes EGFR/Ras signaling in the eye, although the molecular mechanisms underlying this function remain to be determined.

In addition to *mo*, several other mutants that overproduce R3/R4 photoreceptors via the transformation of mystery cells have been identified. These mutants include *fat facets* (*faf*; FISCHER-VIZE *et al.* 1992a), *liquid facets* (*lqf*; FISCHER-VIZE *et al.* 1992b), *sidekick* (*sdk*; NGUYEN *et al.* 1997), *groucho* (*gro*; FISCHER-VIZE *et al.* 1992b), and *strawberry notch* (*sno*; COYLE-THOMPSON and BANERJEE 1993). Unlike *mo*, both *sno* and *sdk* mutant eyes show a reduction in the number of cone cells (NGUYEN *et al.* 1997; TSUDA *et al.* 2002), while the effects of *faf*, *lqf*, and *gro* on the nonneural cone and pigment cells are unknown. Like *mo* and *aos*, R3/R4 production is non-cell autonomously regulated by *faf*, *lqf*, *sdk*, and *gro*. The FAF and LQF proteins are believed to regulate endocytosis, possibly resulting in the downregulation of secreted factors that specify R3/R4, or for the transport of an unknown inhibitory ligand through the cell (CHEN *et al.* 2002). SDK is a transmembrane protein that itself could be a signal that restricts R3/R4 cell fate (NGUYEN *et al.* 1997). No relationship has been established between *lqf*, *sdk*, *gro*, and the Ras pathway. Genetic interactions have been observed between *faf* and *Ras1* in the eye (LI *et al.* 1997). However, the critical time point for this interaction appears to be after R3/R4 specification, and the molecular basis of this interaction is unknown. Thus, it is possible that multiple pathways restrict the formation of R3/R4.

In the process of examining *mo* mutant eye clones from adult retinas, genetically wild-type ommatidia that

contain an extra photoreceptor were found. In addition to showing that *mo* can function through a non-cell-autonomous mechanism, this result also suggests that R3/R4 formation is regulated by long-range signals that arise outside of the nascent ommatidium. Such a group of cells might be found in more mature ommatidia located posterior to the region of R3/R4 specification. Another possibility is that R3/R4 specification is regulated by production of Argos in the peripodium, a squamous epithelial layer that lies along the apical surface of the eye disc neuroepithelium. The importance of the peripodium for the presentation of signaling ligands throughout multiple stages of eye development is well established (CHO *et al.* 2000; GIBSON and SCHUBIGER 2000), and delivery of Argos during the R3/R4 specification step may be one of its functions. While it is still unknown how these phenotypically mutant but genotypically wild-type ommatidia arise, the occurrence of similar ommatidia has been observed in mutants of *aos* (FREEMAN *et al.* 1992b), *gro* (FISCHER-VIZE *et al.* 1992b), and *lqf* (CADAVID *et al.* 2000). The observation of this phenomenon in multiple mutants shows that it is not specific to *mo*. Rather, these data indicate that R3/R4 specification is regulated remotely, potentially by multiple signaling pathways.

While studies of the *mo* embryonic phenotype were uninformative in terms of determining whether *mo* functions as an EGFR pathway antagonist outside of the eye, the aristapedia phenotype from which the gene derives its name may provide a suitable context for such analyses in the future. Although we are not aware of any examples in which hyperactivation of the EGFR pathway results in arista-to-leg transformations, it has been shown that EGFR activation specifies the distal region of the leg by preventing expression of the genes *rotund* and *bric-a-brac* in the presumptive tarsal region (GALINDO *et al.* 2002). In this context, EGFR antagonizes the activity of the transcription factor Distal-less (Dll), which activates expression of *rotund* and *bric-a-brac* in a more medial region of the leg imaginal disc. This relationship between EGFR and Dll in the leg could also be invoked to explain the aristapedia phenotype seen in *mo* mutant clones. Consistent with such speculation, it has been shown that weak hypomorphic combination of *Dll* alleles results in an aristapedia phenotype (DONG *et al.* 2000). Thus, perhaps hyperactivation of EGFR, as a consequence of loss of *mo* function, could produce the same result by more effectively or broadly antagonizing the activity of Dll in the presumptive arista. Again, this model is purely speculative because such a role for EGFR in the arista has not been established.

The N terminus of RNO is highly conserved in related proteins across several species. This conserved region contains a PHD finger, a motif most often found in proteins that participate in chromatin-remodeling complexes (AASLAND *et al.* 1995). Further supporting the notion that it may function as a transcriptional regulator, RNO is localized to the nucleus.

Recent reports have heightened our understanding of how PHD domains function at a molecular level. Each PHD motif coordinates two zinc ions in a structure very similar to that of the RING finger (BORDEN and FREEMONT 1996; PASCUAL *et al.* 2000). Several RING finger proteins regulate protein stability as members of E3 ubiquitin ligase complexes (JOAZEIRO and WEISSMAN 2000), and researchers have begun to test PHD domains for ubiquitin ligase activity on the basis of structural similarity of the two domains. For example, mammalian MEKK1, which is best known as a MAPKKK in the mammalian MAPK pathways, contains a PHD domain that allows it to mediate the ubiquitination and downregulation of the ERK MAPK in response to extracellular stress (LU *et al.* 2002). Another example can be found in the MIR2 protein of the Karposi's sarcoma-associated herpes virus. Evidence strongly suggests that the PHD domain of MIR2 mediates the ubiquitination of host defense molecules, causing their endocytosis and subsequent destruction (COSCOY *et al.* 2001; LORENZO *et al.* 2002). These insights into the biochemical activity of PHD domain proteins suggest that they may mediate ubiquitination of proteins that affect chromatin architecture or transcription. Ubiquitination is an important mechanism for regulating the activities of chromatin-associated proteins such as histones, RNAPoIII, and transcription factors via proteolytic and nonproteolytic pathways (reviewed in CONAWAY *et al.* 2002; MURATANI and TANSEY 2003). Given the abundance of PHD fingers found in chromatin-remodeling complexes, the possibility that many of them participate in ubiquitination is of great potential interest.

The three most closely related homologs to RNO in humans are KIAA0215, JADE-1, and KIAA0239. No publications describe the functions of KIAA0215 or KIAA0239. JADE-1 was identified as a physical interactor of the von Hippel-Lindau (VHL) tumor suppressor by yeast two-hybrid analyses and this interaction was confirmed by co-immunoprecipitation studies (ZHOU *et al.* 2002). The N terminus of JADE-1, preceding the PHD region, is essential for this interaction and is conserved in RNO (39% identical and 61% similar to aa 1–203 of JADE-1). Given that RNO is the closest homolog to JADE-1 in *Drosophila*, it seems possible that RNO may physically interact with the *Drosophila* homolog of VHL (ADRYAN *et al.* 2000). Intriguingly, immunoprecipitates of endogenous VHL have been shown to contain ubiquitin ligase activity (LISZTIAN *et al.* 1999). Furthermore, this activity appears important for VHL function because it is abrogated by tumorigenic changes in the VHL sequence (LISZTIAN *et al.* 1999). These observations suggest that JADE-1, and by extension RNO, may participate in E3 ubiquitin ligase complexes, as has been reported for other PHD fingers.

In conclusion, we have phenotypically characterized and molecularly identified a novel gene, *rhinoceros*,

which regulates the specification of cell fates during ommatidial assembly in *Drosophila*. On the basis of combined genetic and molecular data presented in this report, we propose that RNO-dependent transcriptional activity is required to modulate expression of key EGFR/Ras pathway regulators and effectors in the developing eye. Such regulation could involve activation of inhibitory factors, such as *argos*, and/or repression of positive regulators. Identification of transcriptional targets of *mo* will likely be essential in elucidating the molecular mechanisms underlying *mo*-mediated antagonism of EGFR pathway activity in the developing eye.

We are indebted to L. Zipursky for *GMR-EbiN*; the Bloomington Stock Center for numerous fly stocks; G. Rubin for *TM3-sew-Ras<sup>v12</sup>*, anti-Rough, anti-Cut, and cDNA libraries; R. Barrio for anti-SALM; and the Developmental Studies Hybridoma Bank for anti-ELAV, anti-Argos, and anti-ARM. We also thank T. Orr-Weaver, P. Garrity, F. Chen, M. Mutsuddi, S. Silver, and T. Tootle for helpful discussions; E. Davies for critical reading of this manuscript; T. Wolff for advice on pupal dissections; and A. Williams for technical support. Confocal and scanning electron microscopy was performed in the W. M. Keck Biological Imaging Facility. M. Voas was supported by a National Institutes of Health (NIH) training grant. This work was supported in part by NIH grant RO1 EY-12549 to I.R.

#### LITERATURE CITED

- AASLAND, R., T. J. GIBSON and A. F. STEWART, 1995 The PHD finger: implications for chromatin-mediated transcriptional regulation. *Trends Biochem. Sci.* **20**: 56–59.
- ADAMS, M. D., S. E. CELNIKER, R. A. HOLT, C. A. EVANS, J. D. GOCAYNE *et al.*, 2000 The genome sequence of *Drosophila melanogaster*. *Science* **287**: 2185–2195.
- ADRYAN, B., H. J. DECKER, T. S. PAPAS and T. HSU, 2000 Tracheal development and the von Hippel-Lindau tumor suppressor homolog in *Drosophila*. *Oncogene* **19**: 2803–2811.
- BATEMAN, A., E. BIRNEY, L. CERRUTI, R. DURBIN, L. ETWILLER *et al.*, 2002 The Pfam protein families database. *Nucleic Acids Res.* **30**: 276–280.
- BORDEN, K. L., and P. S. FREEMONT, 1996 The RING finger domain: a recent example of a sequence-structure family. *Curr. Opin. Struct. Biol.* **6**: 395–401.
- BRAND, A. H., and N. PERRIMON, 1993 Targeted gene expression as a means of altering cell fates and generating dominant phenotypes. *Development* **118**: 401–415.
- CADAVID, A. L., A. GINZEL and J. A. FISCHER, 2000 The function of the *Drosophila* fat facets deubiquitinating enzyme in limiting photoreceptor cell number is intimately associated with endocytosis. *Development* **127**: 1727–1736.
- CHEN, X., B. ZHANG and J. A. FISCHER, 2002 A specific protein substrate for a deubiquitinating enzyme: liquid facets is the substrate of fat facets. *Genes Dev.* **16**: 289–294.
- CHO, K. O., J. CHERN, S. IZADDOOST and K. W. CHOI, 2000 Novel signaling from the peripodial membrane is essential for eye disc patterning in *Drosophila*. *Cell* **103**: 331–342.
- CONAWAY, R. C., C. S. BROWER and J. W. CONAWAY, 2002 Emerging roles of ubiquitin in transcription regulation. *Science* **296**: 1254–1258.
- COOPER, M. T., and S. J. BRAY, 2000 R7 photoreceptor specification requires Notch activity. *Curr. Biol.* **10**: 1507–1510.
- COSCOY, L., D. J. SANCHEZ and D. GANEM, 2001 A novel class of herpesvirus-encoded membrane-bound E3 ubiquitin ligases regulates endocytosis of proteins involved in immune recognition. *J. Cell Biol.* **155**: 1265–1274.
- COYLE-THOMPSON, C. A., and U. BANERJEE, 1993 The *strawberry notch* gene functions with *Notch* in common developmental pathways. *Development* **119**: 377–395.
- DE NOOIJ, J. C., and I. K. HARIHARAN, 1995 Uncoupling cell fate

- determination from patterned cell division in the *Drosophila* eye. *Science* **270**: 983–985.
- DONG, P. D., J. CHU and G. PANGANIBAN, 2000 Coexpression of the homeobox genes *Distal-less* and *homothorax* determines *Drosophila* antennal identity. *Development* **127**: 209–216.
- DONG, X., L. TSUDA, K. H. ZAVITZ, M. LIN, S. LI *et al.*, 1999 *ebi* regulates epidermal growth factor receptor signaling pathways in *Drosophila*. *Genes Dev.* **13**: 954–965.
- FAIR, K., M. ANDERSON, E. BULANOVA, H. MI, M. TROPSCHUG *et al.*, 2001 Protein interactions of the MLL PHD fingers modulate MLL target gene regulation in human cells. *Mol. Cell. Biol.* **21**: 3589–3597.
- FEHON, R. G., P. J. KOOH, I. REBAY, C. L. REGAN, T. XU *et al.*, 1990 Molecular interactions between the protein products of the neurogenic loci *Notch* and *Delta*, two EGF-homologous genes in *Drosophila*. *Cell* **61**: 523–534.
- FISCHER-VIZE, J. A., G. M. RUBIN and R. LEHMANN, 1992a The fat facets gene is required for *Drosophila* eye and embryo development. *Development* **116**: 985–1000.
- FISCHER-VIZE, J. A., P. D. VIZE and G. M. RUBIN, 1992b A unique mutation in the Enhancer of split gene complex affects the fates of the mystery cells in the developing *Drosophila* eye. *Development* **115**: 89–101.
- FREEMAN, M., 1994a Misexpression of the *Drosophila* *argos* gene, a secreted regulator of cell determination. *Development* **120**: 2297–2304.
- FREEMAN, M., 1994b The *spitz* gene is required for photoreceptor determination in the *Drosophila* eye where it interacts with the EGF receptor. *Mech. Dev.* **48**: 25–33.
- FREEMAN, M., 1996 Reiterative use of the EGF receptor triggers differentiation of all cell types in the *Drosophila* eye. *Cell* **87**: 651–660.
- FREEMAN, M., 1997 Cell determination strategies in the *Drosophila* eye. *Development* **124**: 261–270.
- FREEMAN, M., 2000 Feedback control of intercellular signalling in development. *Nature* **408**: 313–319.
- FREEMAN, M., B. E. KIMMEL and G. M. RUBIN, 1992a Identifying targets of the rough homeobox gene of *Drosophila*: evidence that rhomboid functions in eye development. *Development* **116**: 335–346.
- FREEMAN, M., C. KLAMBT, C. S. GOODMAN and G. M. RUBIN, 1992b The *argos* gene encodes a diffusible factor that regulates cell fate decisions in the *Drosophila* eye. *Cell* **69**: 963–975.
- GALINDO, M. I., S. A. BISHOP, S. GREIG and J. P. COUSO, 2002 Leg patterning driven by proximal-distal interactions and EGFR signaling. *Science* **297**: 256–259.
- GAUL, U., G. MARDON and G. M. RUBIN, 1992 A putative Ras GTPase activating protein acts as a negative regulator of signaling by the Sevenless receptor tyrosine kinase. *Cell* **68**: 1007–1019.
- GIBSON, M. C., and G. SCHUBIGER, 2000 Peripodial cells regulate proliferation and patterning of *Drosophila* imaginal discs. *Cell* **103**: 343–350.
- GOLEMO, M., R. SCHWEITZER, M. FREEMAN and B. Z. SHILO, 1996 *Argos* transcription is induced by the *Drosophila* EGF receptor pathway to form an inhibitory feedback loop. *Development* **122**: 223–230.
- HAYASHI, T., and K. SAIGO, 2001 Diversification of cell types in the *Drosophila* eye by differential expression of prepatterning genes. *Mech. Dev.* **108**: 13–27.
- HOLT, R. A., G. M. SUBRAMANIAN, A. HALPERN, G. G. SUTTON, R. CHARLAB *et al.*, 2002 The genome sequence of the malaria mosquito *Anopheles gambiae*. *Science* **298**: 129–149.
- ISSHIKI, T., B. PEARSON, S. HOLBROOK and C. Q. DOE, 2001 *Drosophila* neuroblasts sequentially express transcription factors which specify the temporal identity of their neuronal progeny. *Cell* **106**: 511–521.
- JIN, M. H., K. SAWAMOTO, M. ITO and H. OKANO, 2000 The interaction between the *Drosophila* secreted protein *argos* and the epidermal growth factor receptor inhibits dimerization of the receptor and binding of secreted *spitz* to the receptor. *Mol. Cell. Biol.* **20**: 2098–2107.
- JOAZEIRO, C. A., and A. M. WEISSMAN, 2000 RING finger proteins: mediators of ubiquitin ligase activity. *Cell* **102**: 549–552.
- KRAMPS, T., O. PETER, E. BRUNNER, D. NELLEN, B. FROESCH *et al.*, 2002 Wnt/wingless signaling requires BCL9/legless-mediated recruitment of pygopus to the nuclear beta-catenin-TCF complex. *Cell* **109**: 47–60.
- LAI, Z. C., and G. M. RUBIN, 1992 Negative control of photoreceptor development in *Drosophila* by the product of the *yan* gene, an ETS domain protein. *Cell* **70**: 609–620.
- LAI, Z. C., S. D. HARRISON, F. KARIM, Y. LI and G. M. RUBIN, 1996 Loss of *tramtrack* gene activity results in ectopic R7 cell formation, even in a *sina* mutant background. *Proc. Natl. Acad. Sci. USA* **93**: 5025–5030.
- LEE, J. R., S. URBAN, C. F. GARVEY and M. FREEMAN, 2001 Regulated intracellular ligand transport and proteolysis control egf signal activation in *Drosophila*. *Cell* **107**: 161–171.
- LI, Q., I. K. HARIHARAN, F. CHEN, Y. HUANG and J. A. FISCHER, 1997 Genetic interactions with Rap1 and Ras1 reveal a second function for the fat facets deubiquitinating enzyme in *Drosophila* eye development. *Proc. Natl. Acad. Sci. USA* **94**: 12515–12520.
- LINDER, B., R. NEWMAN, L. K. JONES, S. DEBERNARDI, B. D. YOUNG *et al.*, 2000 Biochemical analyses of the AF10 protein: the extended LAP/PHD-finger mediates oligomerisation. *J. Mol. Biol.* **299**: 369–378.
- LISZTWAN, J., G. IMBERT, C. WIRBELAUER, M. GSTAIGER and W. KREK, 1999 The von Hippel-Lindau tumor suppressor protein is a component of an E3 ubiquitin-protein ligase activity. *Genes Dev.* **13**: 1822–1833.
- LORENZO, M. E., J. U. JUNG and H. L. PLOEGH, 2002 Kaposi's sarcoma-associated herpesvirus K3 utilizes the ubiquitin-proteasome system in routing class major histocompatibility complexes to late endocytic compartments. *J. Virol.* **76**: 5522–5531.
- LU, Z., S. XU, C. JOAZEIRO, M. H. COBB and T. HUNTER, 2002 The PHD domain of MEKK1 acts as an E3 ubiquitin ligase and mediates ubiquitination and degradation of ERK1/2. *Mol. Cell* **9**: 945–956.
- MCCONNELL, S. K., 1989 The determination of neuronal fate in the cerebral cortex. *Trends Neurosci.* **12**: 342–349.
- MILLER, D. T., and R. L. CAGAN, 1998 Local induction of patterning and programmed cell death in the developing *Drosophila* retina. *Development* **125**: 2327–2335.
- MULDER, N. J., R. APWEILER, T. K. ATTWOOD, A. BAIROCH, D. BARRELL *et al.*, 2003 The InterPro Database, 2003 brings increased coverage and new features. *Nucleic Acids Res.* **31**: 315–318.
- MURATANI, M., and W. P. TANSEY, 2003 How the ubiquitin-proteasome system controls transcription. *Nat. Rev. Mol. Cell. Biol.* **4**: 192–201.
- NEWSOME, T. P., B. ASLING and B. J. DICKSON, 2000 Analysis of *Drosophila* photoreceptor axon guidance in eye-specific mosaics. *Development* **127**: 851–860.
- NGUYEN, D. N., Y. LIU, M. L. LITSKY and R. REINKE, 1997 The *sidekick* gene, a member of the immunoglobulin superfamily, is required for pattern formation in the *Drosophila* eye. *Development* **124**: 3303–3312.
- O'CONNELL, S., L. WANG, S. ROBERT, C. A. JONES, R. SAINT *et al.*, 2001 Polycomblike PHD fingers mediate conserved interaction with enhancer of zeste protein. *J. Biol. Chem.* **276**: 43065–43073.
- PASCUAL, J., M. MARTINEZ-YAMOUT, H. J. DYSON and P. E. WRIGHT, 2000 Structure of the PHD zinc finger from human Williams-Beuren syndrome transcription factor. *J. Mol. Biol.* **304**: 723–729.
- PIGNONI, F., and S. L. ZIPURSKY, 1997 Induction of *Drosophila* eye development by decapentaplegic. *Development* **124**: 271–278.
- REBAY, I., 2002 Keeping the receptor tyrosine kinase signaling pathway in check: lessons from *Drosophila*. *Dev. Biol.* **251**: 1–17.
- REBAY, I., and R. G. FEHON, 2000 Generating antibodies against *Drosophila* proteins, pp. 389–411 in *Drosophila Protocols*, edited by W. SULLIVAN, M. ASHBURNER and R. S. HAWLEY. Cold Spring Harbor Laboratory Press, Cold Spring Harbor, NY.
- REBAY, I., F. CHEN, F. HSIAO, P. A. KOLODZIEJ, B. H. KUANG *et al.*, 2000 A genetic screen for novel components of the Ras/Mitogen-activated protein kinase signaling pathway that interact with the *yan* gene of *Drosophila* identifies split ends, a new RNA recognition motif-containing protein. *Genetics* **154**: 695–712.
- SAHA, V., T. CHAPLIN, A. GREGORINI, P. AYTON and B. D. YOUNG, 1995 The leukemia-associated-protein (LAP) domain, a cysteine-rich motif, is present in a wide range of proteins, including MLL, AF10, and MLLT6 proteins. *Proc. Natl. Acad. Sci. USA* **92**: 9737–9741.
- SCHWEITZER, R., R. HOWES, R. SMITH, B. Z. SHILO and M. FREEMAN,

- 1995 Inhibition of *Drosophila* EGF receptor activation by the secreted protein Argos. *Nature* **376**: 699–702.
- SPENCER, S. A., P. A. POWELL, D. T. MILLER and R. L. CAGAN, 1998 Regulation of EGF receptor signaling establishes pattern across the developing *Drosophila* retina. *Development* **125**: 4777–4790.
- TIO, M., and K. MOSES, 1997 The *Drosophila* TGF alpha homolog Spitz acts in photoreceptor recruitment in the developing retina. *Development* **124**: 343–351.
- TIO, M., C. MA and K. MOSES, 1994 *spitz*, a *Drosophila* homolog of transforming growth factor-alpha, is required in the founding photoreceptor cells of the compound eye facets. *Mech. Dev.* **48**: 13–23.
- TOMLINSON, A., and G. STRUHL, 2001 Delta/Notch and Boss/Sevenless signals act combinatorially to specify the *Drosophila* R7 photoreceptor. *Mol. Cell* **7**: 487–495.
- TSUDA, L., R. NAGARAJ, S. ZIPURSKY and U. BANERJEE, 2002 An EGFR/Ebi/Sno pathway promotes delta expression by inactivating Su(H)/SMRTER repression during inductive Notch signaling. *Cell* **110**: 625.
- URBAN, S., J. R. LEE and M. FREEMAN, 2001 *Drosophila* rhomboid-1 defines a family of putative intramembrane serine proteases. *Cell* **107**: 173–182.
- WOLFF, T., 2000 Histological techniques for the *Drosophila* eye part I: larva and pupa, pp. 201–227 in *Drosophila Protocols*, edited by W. SULLIVAN, M. ASHBURNER and R. S. HAWLEY. Cold Spring Harbor Laboratory Press, Cold Spring Harbor, NY.
- WOLFF, T., and D. F. READY, 1991 Cell death in normal and rough eye mutants of *Drosophila*. *Development* **113**: 825–839.
- WOLFF, T., and D. F. READY, 1993 Pattern formation in the *Drosophila* retina, pp. 1277–1325 in *The Development of Drosophila melanogaster*, edited by M. BATE and A. MARTINEZ-ARIAS. Cold Spring Harbor Laboratory Press, Cold Spring Harbor, NY.
- XU, T., and G. M. RUBIN, 1993 Analysis of genetic mosaics in developing and adult *Drosophila* tissues. *Development* **117**: 1223–1237.
- ZHOU, M. I., H. WANG, J. J. ROSS, I. KUZMIN, C. XU *et al.*, 2002 The von Hippel-Lindau tumor suppressor stabilizes novel plant homeodomain protein Jade-1. *J. Biol. Chem.* **277**: 39887–39898.

Communicating editor: K. ANDERSON